Microfluidics

DOI: 10.1002/anie.200801360

Droplet-Based Microreactors for the Synthesis of Magnetic Iron Oxide Nanoparticles**

Lucas Frenz, Abdeslam El Harrak, Matthias Pauly, Sylvie Bégin-Colin, Andrew D. Griffiths, and Jean-Christophe Baret**

Microfluidic systems are a powerful tool to study and optimize a wide range of biological and chemical reactions,[1] and their use for the synthesis of nanoparticles is attracting more and more attention. Compared to conventional bulk synthesis strategies, microfluidic systems allow more precise control of the reaction conditions, which can lead to reductions in particle size and polydispersity.[2] A range of different nanoparticles have been synthesized in microfluidic systems: CdSe, CdS, TiO_2, boehmite, Au, Co, Ag, Pd, Cu, $BaSO_4$, and CdSe–ZnS core–shell nanoparticles.[2,3] Although there are some recent preliminary results on the synthesis of iron oxide nanoparticles in a millifluidic system,[4] to date a microfluidic synthesis of iron oxide nanoparticles has not been demonstrated. Spinel iron oxide nanocrystals have attracted attention for their use as high-density data storage media,[5] or in biomedical applications, for example as contrast enhancement agents for magnetic resonance imaging (MRI) and for drug delivery.[6,7] Controlling the synthesis conditions of these particles is critical, as these determine their physical properties.[8]

While single-phase microfluidic systems are subjected to diffusion-limited mixing and reagent dispersion, droplet-based microfluidic systems overcome these limitations by fast mixing in spatially isolated microreactors (droplets) containing well-defined quantities of materials[9–11] and therefore provide a high level of control of the synthesis conditions.[12,13] In droplet-based microfluidic systems, reagents are generally brought together in a co-flowing stream just before droplet formation; the reaction occurs later in the microdroplet.[9] However, this method is unsuitable for aggressive or fast reactions, which generate precipitates. To study and control such reactions, it is necessary to initiate the reaction by fusion of two droplets, each containing different reagents. The main limitation is then the accurate pairing of these droplets, which is hindered by small variations in the channel depths or flow rates.[14] There have been attempts to synchronize droplets based on fluidic ladder networks,[15] but the most promising approach is to use a synchronization mechanism directly at the production nozzle. Therefore, strategies such as active control of droplet release using electric fields[16] or passive hydrodynamic coupling at a single nozzle have been proposed.[17,18] Nevertheless, these approaches lack the control of droplet volume ratios required to optimize reaction stoichiometry, and undesired coalescence occurs for certain flow rate regimes.

We present herein an extremely reliable method to create droplet pairs based on hydrodynamic coupling of two spatially separated nozzles. We demonstrate the utility of this system by precipitating iron oxide nanoparticles in a very fast (millisecond) and reproducible reaction after fusion of droplet pairs by electrocoalescence.[14]

[*] L. Frenz, Dr. A. El Harrak, Prof. A. D. Griffiths, Dr. J.-C. Baret
Institut de Science et d'Ingénierie Supramoléculaires (ISIS)
Université Louis Pasteur, CNRS UMR 7006
8, allée Gaspard Monge, BP 70028
67083 Strasbourg Cedex (France)
Fax: (+33) 3-9024-5115
E-mail: griffiths@isis.u-strasbg.fr
jc.baret@isis.u-strasbg.fr
M. Pauly, Prof. S. Bégin-Colin
Institut de Physique et Chimie des Matériaux (IPCMS)
Université Louis Pasteur, CNRS UMR 7504
23, rue du Loess, BP 43, 67034 Strasbourg Cedex 2 (France)

[**] We thank D. A. Weitz, D. Link, and the members of Raindance Technologies for their support, as well as P. Schultz, M. Erhardt, and C. Ulhaq-Bouillet for their help with the TEM and A. Derory for the magnetic measurements. L.F. was supported by the EC FP6 Marie Curie Research Training Network, ProSA, A.E.H. by the EC FP6 project MiFem, M.P. by the DGA (Direction Générale de l'Armement) and J.-C.B. by an EMBO long-term fellowship [ALTF 915-2006]. This work was also supported by the Ministère de l'Enseignement Supérieur et de la Recherche, CNRS, and ANR [ANR-05-BLAN-0397].

Supporting information for this article is available on the WWW under http://dx.doi.org/10.1002/anie.200801360.

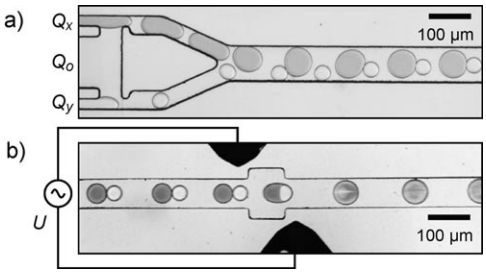

Figure 1. a) Pairing module. Two aqueous phases are injected by the outer channels and are synchronously emulsified by the central oil channel. The flow rates are $Q_o = 800\ \mu L\,h^{-1}$ for the oil and $Q_x = 400\ \mu L\,h^{-1}$, $Q_y = 100\ \mu L\,h^{-1}$ for the aqueous phases. b) Fusion module. Paired droplets can be coalesced by applying an electrical voltage U between the two electrodes. $Q_o = 650\ \mu L\,h^{-1}$, $Q_x = 100\ \mu L\,h^{-1}$, $Q_y = 60\ \mu L\,h^{-1}$. The corresponding movies M1 and M2 are provided in the Supporting Information.

The microfluidic device (Figure 1a) consists of two hydrodynamically coupled nozzles. During droplet formation in one of the nozzles, the aqueous stream blocks the oil

coming from the central channel, leading to an increased oil flow through the second nozzle. Once the droplet is released, the oil flow switches back to the first channel, allowing droplet formation at the second nozzle. This alternation of the oil flow leads to perfect one-by-one droplet pairing at various flow rates. Quantitative analysis was performed by labeling the droplets with different fluorophores in the two aqueous streams (see Figure S1 in the Supporting Information). One nozzle created droplets containing 10 μM fluorescein, the other created droplets containing 50 μM resorufin. Evaluation of the fluorescent signals showed the reliability of pairing to be at least 99.99% over millions of droplets (see Table 1).

Table 1: Examples of long-term stability tests at different flow rate combinations.[a]

Q_o [μL h^{-1}]	Q_x [μL h^{-1}]	Q_y [μL h^{-1}]	$n_{droplets}$	t [min]	f [s^{-1}]	unpaired	error
400	50	30	226 800	15.7	120.22	10	4×10^{-5}
500	100	60	4 019 100	124.7	268.58	22	5×10^{-6}
800	200	100	1 224 300	15.1	675.72	4	3×10^{-6}
800	250	200	2 252 501	23.3	806.11	3	1×10^{-6}
800	500	100	3 711 800	30.7	1007.62	39	1×10^{-5}

[a] Q_o is the oil flow rate and Q_x, Q_y the aqueous flow rates. The error is the ratio of unpaired events to the total number of droplets ($n_{droplets}$) with the measuring time t. f is the droplet generation frequency at each nozzle.

Furthermore, droplet pairing is not only stable at equal aqueous flow rates but also at flow rate ratios up to 1:5. Stoichiometry modulations (1:25) can therefore easily be achieved, since the flow-rate ratio is equal to the droplet volume ratio in this system. (A detailed physical analysis of the pairing will be published elsewhere).

To start a reaction, the droplet pairs can be coalesced by applying an electrical field between the two on-chip electrodes (Figure 1b). Using a co-flow system, mixing in droplets is limited to each droplet hemisphere (Figure 2a),[19] which makes additional mixing modules necessary.[9] In-line droplet fusion (Figures 1b and 2b) overcomes this limitation, since the second compound is injected homogenously into each hemisphere. Furthermore, the dynamical rupture of the interface and the formation of the new droplet assist the mixing.[10]

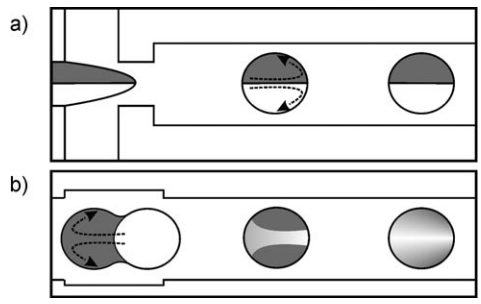

Figure 2. Mixing in droplets. a) Reagents are brought together by a co-flow and then emulsified. Mixing occurs across the central line by diffusion only (ca. 100–1000 ms). b) In-line droplet fusion. Compounds are injected into both droplet hemispheres; mixing is enhanced by convection, which results in faster mixing times (ca. 2 ms).

We have used this system to synthesize magnetic spinel iron oxide nanoparticles by coprecipitation of Fe^{II} and Fe^{III} salt solutions by the addition of a base. This procedure leads first to magnetite (Fe_3O_4), which readily oxidizes to maghemite (γ-Fe_2O_3) on contact with air.[7,8] The coprecipitation is so fast that it immediately forms particles that block the channels in a co-flow system, especially at higher concentrations (data not shown). Droplet fusion can potentially overcome this problem,[18] but in the absence of surfactant,[18] it is extremely difficult to achieve controlled pairwise droplet fusion.[20] In our system, the two aqueous components never mix unintentionally, as the nozzles are spatially separated and the droplets are stabilized by surfactant. Controlled pairwise droplet fusion is achieved by electrocoalescence. This approach enabled us to increase the compound concentration by two to three orders of magnitude compared to earlier droplet-based microfluidic methods for the synthesis of nanoparticles.[18,21] In detail, iron chloride solution was flushed into one arm of the nozzle and ammonium hydroxide into the second arm, which led to droplet pairs containing the two reagents. After electrocoalescence, a precipitate of iron oxide nanoparticles appeared within approximately 2 ms (Figure 3). Because of the identical reaction conditions in all droplets, the kinetics of precipitation and precipitate morphology was extremely similar in all droplets throughout the whole experiment.

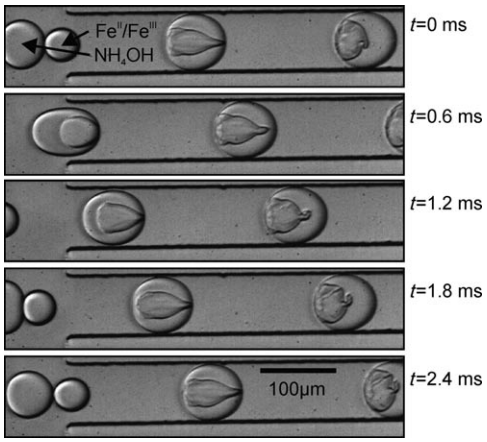

Figure 3. Formation of iron oxide precipitates after coalescence of pairs of droplets. $Q_o = 650$ μL h^{-1} (oil), $Q_x = 60$ μL h^{-1} (iron chloride solution S1, see the Experimental Section), and $Q_y = 120$ μL h^{-1} (ammonium hydroxide). The corresponding movie M3 is provided in the Supporting Information.

Particle-size measurements by transmission electron microscopy (TEM, Figure 4a) show that the average particle diameter is smaller for the fast microfluidic compound mixing (4 ± 1 nm) than for bulk mixing (9 ± 3 nm). Moreover, high-resolution TEM (HRTEM) measurements (inset Figure 4a) show that the nanoparticles are monocrystalline, and no stacking faults are visible. The nanoparticles exhibit planes with interplanar distances of about 0.3 nm, characteristic of

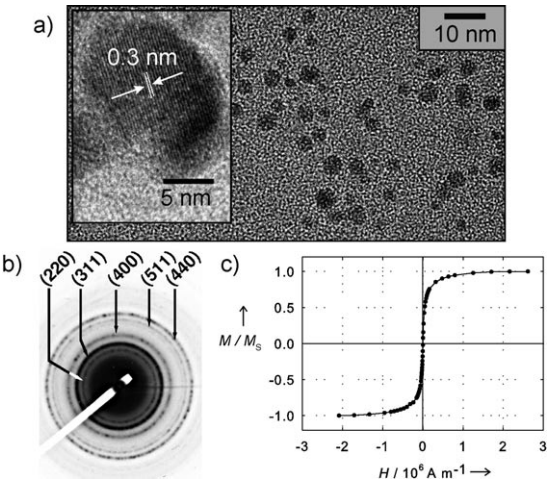

Figure 4. Characterization of the iron oxide particles produced with solution S2 (see the Experimental Section). a) TEM image of the nanoparticles. Inset: HRTEM image of a particle showing (220) spinel planes. b) Electron diffraction pattern indicating different planes of the spinel structure. c) Magnetization M/M_s (M_s is the saturation magnetization) as a function of the magnetic field H.

(220) spinel planes. The electron diffraction pattern measured from a large zone (Figure 4b) confirms the iron oxide spinel structure. Finally, the absence of hysteresis in the magnetization curve (Figure 4c) of the nanoparticles indicates that they are superparamagnetic, which is characteristic of spinel iron oxide nanoparticles smaller than 15 nm.

In summary, we have demonstrated for the first time the synthesis of spinel magnetic iron oxide nanoparticles in a microfluidic system. The novelty of this approach lies in the fact that the reaction is compartmentalized in microdroplets, which function as independent microreactors. We have designed a robust and flexible microfluidic module for the controlled production of droplet pairs based on hydrodynamic coupling, with errors of pairing on the order of only 10^{-5}. The reagents in the droplet pairs are brought together on demand by in-line electrocoalescence, resulting in fast mixing (ca. 2 ms). Various chemical strategies have been developed to obtain magnetic iron oxide particles, sometimes with high monodispersity.[7] The size of nanoparticles synthesized with microfluidics (4 nm) is equal to that of the smallest particles synthesized by other techniques. Furthermore, such on-chip-synthesized particles could potentially be functionalized by an additional droplet-fusion step to synthesize core–shell particles optimized for biocompatibility, drug anchoring, and cell targeting.[22] For iron oxide, these applications are of special interest, as magnetite (Fe_3O_4), which displays a higher saturation magnetization than maghemite (γ-Fe_2O_3), could then be preserved without oxidation. Besides these applications, we believe that this system can be used to control and study a wide range of millisecond kinetic reactions in chemistry and biology and is therefore an additional tool that complements the other pre-existing microfluidic modules for droplet manipulation.

Experimental Section

The 25-μm-deep structures used for fluid channels and electrodes were patterned into poly(dimethylsiloxane) (PDMS) using soft lithography.[23] Electrodes used for fusion were patterned into the same layer in close vicinity to the fluidic channels.[24] A commercial surface coating agent (Aquapel, PPG Industries) was used to coat the channels. Harvard Apparatus syringe pumps (PHD2000) controlled the flow rates. The continuous oil phase was a perfluorocarbon oil FC40 (3M) with 2.5 wt% surfactant made of the ammonium salt of a perfluorinated polyether (PFPE; Krytox FSL–Dupont),[25] stabilizing droplets against coalescence. As starting materials for the precipitation of iron oxide nanoparticles, we used $FeCl_2{\cdot}4H_2O$ (Sigma–Aldrich) and $FeCl_3{\cdot}6H_2O$ (Acros Organics), ammonium hydroxide solution (28% NH_3, Fluka), and hydrochloric acid (37% HCl, Acros Organics) of analytical grade. After degassing 0.5 M HCl in Milli-Q water with an argon flux for 1 h, we added the iron chloride salts and kept this solution under argon. Two different solutions with $Fe^{III}/Fe^{II} = 2{:}1$ ratio were tested: 480 mM $FeCl_3$ + 240 mM $FeCl_2$ (S1) and 60 mM $FeCl_3$ + 30 mM $FeCl_2$ (S2). As a base, we used a 2 M ammonium hydroxide solution, which was also prepared using degassed Milli-Q water. To avoid oxidation of Fe^{II} during the reaction process, the PDMS device was kept in a vacuum chamber overnight before use, the oil was degassed with a nitrogen flux for 1 h, and we used gas-impermeable polyethylene tubing (Becton Dickinson) and collected the sample in a nitrogen atmosphere. Electrocoalescence was achieved by an AC voltage of $U = 200$ V (peak to peak) at 30 kHz, which was applied across the two electrodes positioned on each side of the microfluidics channel. TEM and HRTEM images were recorded with a TOPCON 002B transmission electron microscope operating at 200 kV with a point-to-point resolution of 0.18 nm. Magnetic measurements were performed using a superconducting quantum interference device (SQUID) magnetometer (Quantum Design MPMS-XL) at 200 K.

Received: March 20, 2008
Published online: July 21, 2008

Keywords: iron oxide · microfluidics · microreactors · nanoparticles · synthesis in droplets

[1] G. M. Whitesides et al., *Nature* **2006**, *442*, 368–418 (see Supporting Information).
[2] S. Krishnadasan, R. J. C. Brown, A. J. deMello, J. C. deMello, *Lab Chip* **2007**, *7*, 1434–1441.
[3] L. H. Hung, A. P. Lee, *J. Med. Biol. Eng.* **2007**, *27*, 1–6.
[4] A. Abou Hassan, O. Sandre, V. Cabuil, P. Tabeling, *Chem. Commun.* **2008**, 1783–1785.
[5] G. Reiss, A. Hutten, *Nat. Mater.* **2005**, *4*, 725–726.
[6] S. Mornet, S. Vasseur, F. Grasset, E. Duguet, *J. Mater. Chem.* **2004**, *14*, 2161–2175.
[7] A.-H. Lu, E. Salabas, F. Schüth, *Angew. Chem.* **2007**, *119*, 1242–1266; *Angew. Chem. Int. Ed.* **2007**, *46*, 1222–1244, and references therein.
[8] T. J. Daou, G. Pourroy, S. Begin-Colin, J. M. Greneche, C. Ulhaq-Bouillet, P. Legare, P. Bernhardt, C. Leuvrey, G. Rogez, *Chem. Mater.* **2006**, *18*, 4399–4404.
[9] H. Song, J. D. Tice, R. F. Ismagilov, *Angew. Chem.* **2003**, *115*, 792–796; *Angew. Chem. Int. Ed.* **2003**, *42*, 768–772.
[10] F. Sarrazin, L. Prat, N. Di Miceli, G. Cristobal, D. R. Link, D. A. Weitz, *Chem. Eng. Sci.* **2007**, *62*, 1042–1048.
[11] B. T. Kelly, J.-C. Baret, V. Taly, A. D. Griffiths, *Chem. Commun.* **2007**, 1773–1788.
[12] H. Song, D. L. Chen, R. F. Ismagilov, *Angew. Chem.* **2006**, *118*, 7494–7516; *Angew. Chem. Int. Ed.* **2006**, *45*, 7336–7356.

[13] S.-Y. Teh, R. Lin, L.-H. Hung, A. P. Lee, *Lab Chip* **2008**, *8*, 198 – 220.
[14] K. Ahn, J. Agresti, H. Chong, M. Marquez, D. A. Weitz, *Appl. Phys. Lett.* **2006**, *88*, 264105.
[15] M. Prakash, N. Gershenfeld, *Science* **2007**, *315*, 832 – 835.
[16] D. R. Link, E. Grasland-Mongrain, A. Duri, F. Sarrazin, Z. Cheng, G. Cristobal, M. Marquez, D. A. Weitz, *Angew. Chem.* **2006**, *118*, 2618 – 2622; *Angew. Chem. Int. Ed.* **2006**, *45*, 2556 – 2560.
[17] B. Zheng, J. D. Tice, R. F. Ismagilov, *Anal. Chem.* **2004**, *76*, 4977 – 4982.
[18] L. H. Hung, K. M. Choi, W. Y. Tseng, Y. C. Tan, K. J. Shea, A. P. Lee, *Lab Chip* **2006**, *6*, 174 – 178.
[19] E. Rio, A. Daerr, B. Andreotti, L. Limat, *Phys. Rev. Lett.* **2005**, *94*, 024503.
[20] N. Brémond, A. Thiam, J. Bibette, *Phys. Rev. Lett.* **2008**, *100*, 024501.
[21] I. Shestopalov, J. D. Tice, R. F. Ismagilov, *Lab Chip* **2004**, *4*, 316 – 321.
[22] F. X. Gu, R. Karnik, A. Z. Wang, F. Alexis, E. Levy-Nissenbaum, S. Hong, R. S. Langer, O. C. Farokhzad, *Nano Today* **2007**, *2*, 14 – 21.
[23] Y. N. Xia, G. M. Whitesides, *Annu. Rev. Mater. Sci.* **1998**, *28*, 153 – 184.
[24] A. C. Siegel, S. S. Shevkoplyas, D. B. Weibel, D. A. Bruzewicz, A. W. Martinez, G. M. Whitesides, *Angew. Chem.* **2006**, *118*, 7031 – 7036; *Angew. Chem. Int. Ed.* **2006**, *45*, 6877 – 6882.
[25] K. P. Johnston, K. Harrison, M. Clarke, S. Howdle, M. Heitz, F. Bright, C. Carlier, T. W. Randolph, *Science* **1996**, *271*, 624.

